Physics of Plasmas

RESEARCH ARTICLE | JUNE 23 2023

# Effect of a central barrier potential on asymmetry-induced transport in a coaxial Malmberg–Penning trap

D. L. Eggleston



*Physics of Plasmas* 30, 062305 (2023)
https://doi.org/10.1063/5.0153208

Physics of Plasmas ARTICLE pubs.aip.org/aip/pop

# Effect of a central barrier potential on asymmetry-induced transport in a coaxial Malmberg–Penning trap

Cite as: Phys. Plasmas **30**, 062305 (2023); doi: 10.1063/5.0153208
Submitted: 5 April 2023 · Accepted: 5 June 2023 ·
Published Online: 23 June 2023



D. L. Eggleston[a)]

## AFFILIATIONS

Physics Department, Occidental College, Los Angeles, California 90041, USA

[a)]Author to whom correspondence should be addressed: dleggles@oxy.edu

## ABSTRACT

Experiments are presented measuring the radial particle flux produced when a central barrier potential is applied to the central ring of a coaxial Malmberg–Penning trap at the same time as the voltages producing the main asymmetry potential $\phi_1(r)\cos(kz)\cos(l\theta-\omega t)$. When a negative DC voltage is applied to the entire central ring, the peak flux produced by the main asymmetry is reduced by a factor $e^{(V_{eff}/1.2)}$, where $V_{eff}$ is the effective applied potential in volts. This barrier potential also increases the frequency of this peak flux. When asymmetric $\pm$ voltages are applied to the two azimuthally divided halves of the central ring, DC voltages increase the radial flux while AC voltages decrease it. It is shown that these asymmetric barrier voltages produce their own transport and that the resulting modification of the plasma may be a factor in changing the observed flux.



## I. INTRODUCTION

The excellent confinement of non-neutral plasmas in Malmberg–Penning traps makes them especially suitable for basic studies of plasma transport. There have been many experiments measuring transport produced by applied electric or magnetic fields that break the cylindrical symmetry of the traps.[1–8] The basic process in such experiment seems clear: the applied asymmetries produce radial drifts which, together with some collisional process, produce radial transport. Connecting the experimental results to a detailed transport theory, however, has proven more difficult. Kabantsev and co-workers[9–14] have made progress in this task by focusing on the role of axially trapped particles. Due to the strong velocity-space gradients associated with trapping, these particles have an enhanced collisionality moving them from axially trapped to untrapped and back. Their work has shown that such particles can have a dominate role in the bulk expansion of the plasma as well as the damping of certain plasma modes. Most of their work uses a slightly tilted magnetic field as the bulk asymmetry, and a symmetric or azimuthally varying barrier voltage ("squeeze") applied to the center of the machine to produce the trapped particle populations, but they have also presented evidence that even weak axial variations in the magnetic field can produce trapped particles via the mirror effect.

The transport experiments at Occidental College are performed in a coaxial version of the Malmberg–Penning trap and use time-varying applied electric field asymmetries to produce radial transport, with the resulting radial particle flux measured as a function of radius. Measurements of this flux as a function of asymmetry frequency give a distinctive set of peaked curves,[7] but our attempts to explain these curves using resonant particle theory[15] have not been successful. Motivated by the above-mentioned work of Kabantsev and co-workers as well as the results of our simple particle simulations,[16–18] we have considered the role of trapped particles in our experiment. In a previous paper, we have shown experimentally that weak axial variations in the magnetic field do not play a role.[19] In this paper, we investigate the effect of adding a barrier potential to the center of the trap. We find that barrier potentials do affect the characteristic flux vs frequency curves, but the interpretation of these changes is unclear.

The paper is organized as follows: Sec. II gives a description of the experimental device and our characteristic flux vs frequency curves. Section III gives the experimental results for various types of barrier potentials. These results are discussed in Sec. IV, leading to clarifying follow-up experiments. Finally, our conclusions are given in Sec. V.

## II. EXPERIMENTAL DEVICE

The experiments presented in this paper are performed in a coaxial Malmberg–Penning trap in which the plasma has been replaced by a biased wire and the transport of low density test particles is studied.[7]

The trap design is shown in Fig. 1. The axial magnetic field $B$ and negatively biased end cylinders of the standard trap design are retained, but the plasma is replaced by a thin biased wire (radius $a = 0.007$ in., wire bias potential denoted as $\phi_{cw}$) suspended along the axis of the trap. This wire provides a radial electric field to replace the field normally produced by the plasma column and allows low density electrons injected into the device to have the same zeroth-order dynamical motions as those in a typical non-neutral plasma (axial bounce and azimuthal $E \times B$ drift motions) while the low density suppresses collective modes and simplifies calculation of the electric field. For these experiments $B = 364$ G and $\phi_{cw} = -80$ V except where noted. The entire confinement region is sectored (five cylinders, labeled S1 through S5 in Fig. 1, with eight azimuthal divisions each). For these experiments, we apply a known asymmetry by selecting the amplitude and phase of the voltages applied to each sector to produce a helical standing wave of the following form:

$$\phi(r, \theta, z, t) = \phi_W \frac{r}{R} \cos\left(\frac{n\pi z}{L}\right) \cos(l\theta - \omega t), \tag{1}$$

where $\phi_W$ is the asymmetry potential at the wall (typically 0.2 V), $R$ is the wall radius (3.82 cm), $L$ is the length of the confinement region (76.8 cm), $n$ and $l$ are the axial and azimuthal Fourier mode numbers, respectively, and here, $z$ is measured from one end of the confinement region. For these experiments, $n = l = 1$. The relative phases of the applied voltages are adjusted so that the asymmetry rotates in the same direction as the zeroth-order azimuthal $E \times B$ drift. Previous experiments[7] have shown that little transport is produced when the asymmetry rotates in the opposite direction.

Electrons are injected into the trap from an off-axis gun and are quickly dispersed into an annular distribution with peak density $\sim 10^5\ \mathrm{cm}^{-3}$ and axial temperature $T \approx 4$ eV, giving a calculated 90 degree electron–electron collision frequency $\nu_{ee} \approx 0.25\ s^{-1}$. At a chosen time (here, 1600 ms after injection), the asymmetries are switched on for a period of time $\delta t$ (here, 100 ms) and then switched off. After a delay (typically 10 ms), the electrons are dumped axially onto a phosphor screen and the resulting image is digitized using a $512 \times 512$ pixel charge-coupled device camera. A radial cut through this image gives the density profile $n_0(r)$ of the electrons. No significant azimuthal variation in $n_0(r)$ is observed. Calibration is provided by a measurement of the total charge being dumped. Profiles are taken both with the asymmetry on and off, and the resulting change in density $\delta n_0(r)$ is obtained. The background transport is typically small compared to the induced transport and is subtracted off. If the asymmetry amplitude is small enough and the asymmetry pulse length $\delta t$ short enough, then $\delta n_0(r)$ will increase linearly in time.[5] We may then approximate $\partial n_0/\partial t \simeq \delta n_0(r)/\delta t$ and integrate the continuity equation $\partial n_0/\partial t + \nabla \cdot \Gamma = 0$ to calculate the radial particle flux $\Gamma(r)$ [assuming $\Gamma(r = a) = 0$],

$$\Gamma(r) = -\frac{1}{r}\int_a^r r' dr' \cdot \frac{\partial n_0}{\partial t}(r'). \tag{2}$$

Here, $a$ is the radius of the central wire. The entire experiment is then repeated for a series of asymmetry frequencies and the resulting flux vs frequency data saved for analysis. Typical data are shown in Fig. 2 reproduced from Ref. 7. Radial flux vs asymmetry frequency is shown for four selected values of radius and three values of the center wire bias. The electron density vs radius is shown in the insets. A detailed empirical study of these characteristic curves is given in Ref. 7, but it should be emphasized that there has not yet been a theoretical explanation of their properties.

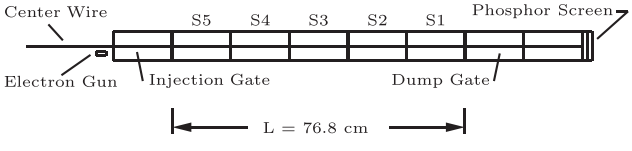


**FIG. 1.** Schematic of the Occidental College trap. The usual non-neutral plasma column is replaced by a biased wire that produces an azimuthal $E \times B$ drift similar to that found in other devices. The five cylinders labeled S1–S5 are divided azimuthally into eight sectors each. These 40 wall sectors are biased to create an asymmetric field that causes radial transport of the low density electrons injected from an off-axis gun.

## III. EXPERIMENTAL RESULTS

The sector biases producing the asymmetry potential given in Eq. (1) (which we will refer to as the *main* asymmetry) leave the sectors of ring S3 grounded. In the current experiments, we use this ring to apply an *additional* voltage, often called a squeeze. We report the effect on our characteristic flux vs asymmetry frequency curves of three types of squeeze: (1) a negative DC squeeze applied to the full ring (azimuthally symmetric DC); (2) equal and opposite DC voltages applied to the two azimuthal halves of the ring (azimuthally asymmetric DC); and (3) equal and opposite AC voltages applied to the two azimuthal halves of the ring at various frequencies (azimuthally asymmetric AC). These squeeze voltages are applied simultaneously with the main asymmetry potential. Although we did not obtain calibration data for these experiments, comparison with the curves of Fig. 2 taken with the same experimental settings gives the approximate result 1000 a.u. $\approx 10^5\ \mathrm{cm}^{-2}\ \mathrm{sec}^{-1}$ for Fig. 3 and those following.

### A. Symmetric DC squeeze

For the first experiment, we use a negative pulsed DC squeeze voltage applied to the entire S3 ring. The effect on the flux vs frequency curves is shown for two representative radii in Fig. 3. For clarity, only some of the curves in our dataset are shown and lines connect the data points to show trends. Three effects are noticeable as the squeeze becomes more negative: the decrease in the peak value of the flux, the increase in the frequency of this peak value, and the change in the overall shape of the flux vs frequency curve.

The decrease in the magnitude of the peak flux value with more negative squeeze voltage is shown in Fig. 4(a), where the peak flux magnitude $|\Gamma_p|$ is plotted vs the magnitude of the squeeze voltage applied to S3 for the two chosen radii. Figure 4(b) shows how the frequency $f_p$ at which the peak flux occurs changes with squeeze voltage. At both radii, the fit curve shows the increase in $f_p$ is linear with the magnitude of the squeeze voltage. The stair-step behavior of the data is an artifact of the limited number of frequencies in the dataset.

If the effect of the squeeze voltage is to form a barrier to electrons moving axially across the device, then the relevant potential is not the voltage $V_{sq}$ applied to S3 but the potential $V_{eff}$ at the chosen radius. This is given by

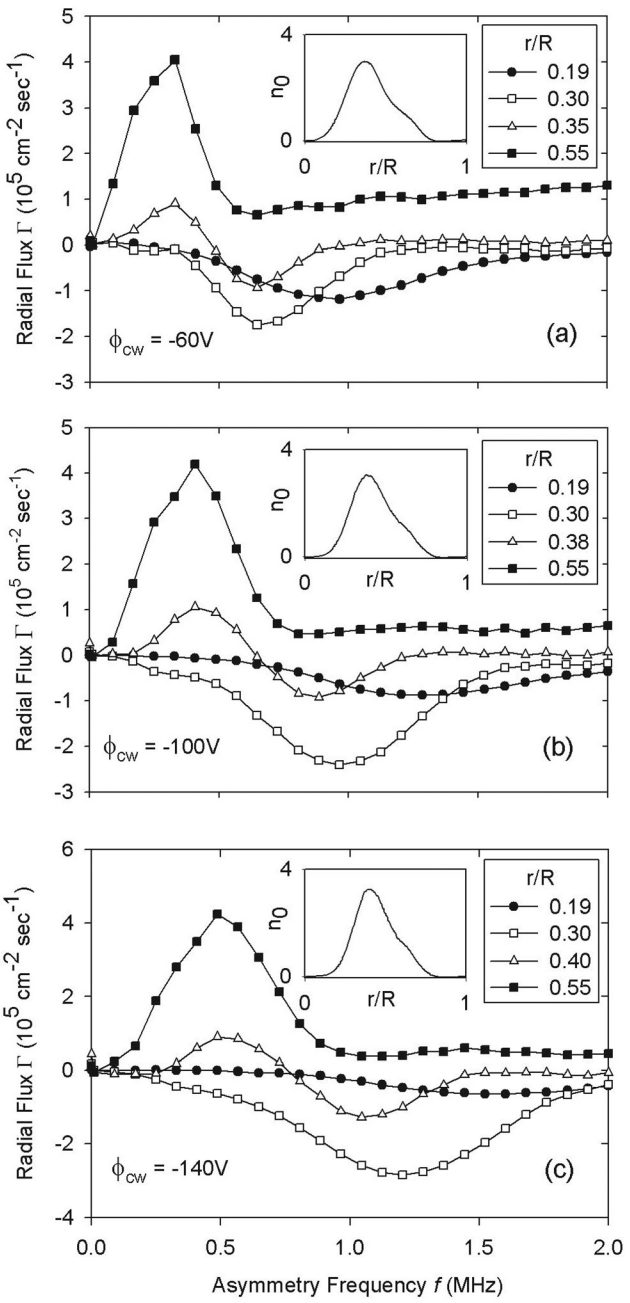


**FIG. 2.** Typical radial flux vs main asymmetry frequency data at selected radial positions for three values of the center wire bias $\phi_{cw}$: (a) $\phi_{cw} = -60$, (b) $\phi_{cw} = -100$, and (c) $\phi_{cw} = -140$ V. The electron density $n_0$ ($10^5$ cm$^{-3}$) vs scaled radius $r/R$ is shown in the inset. Reproduced from D.L. Eggleston and B. Carrillo, Phys. Plasmas **10**, 1308 (2003) with the permission of AIP Publishing.

$$V_{eff} = V_{sq} \ln(r/a) / \ln(R/a). \quad (3)$$

In Fig. 5, we plot the logarithm of $|\Gamma_p|$ vs the effective barrier potential $V_{eff}$. The solid lines show that the decrease in $|\Gamma_p|$ is roughly exponential with $V_{eff}$ with a scale factor of 1.2 V.

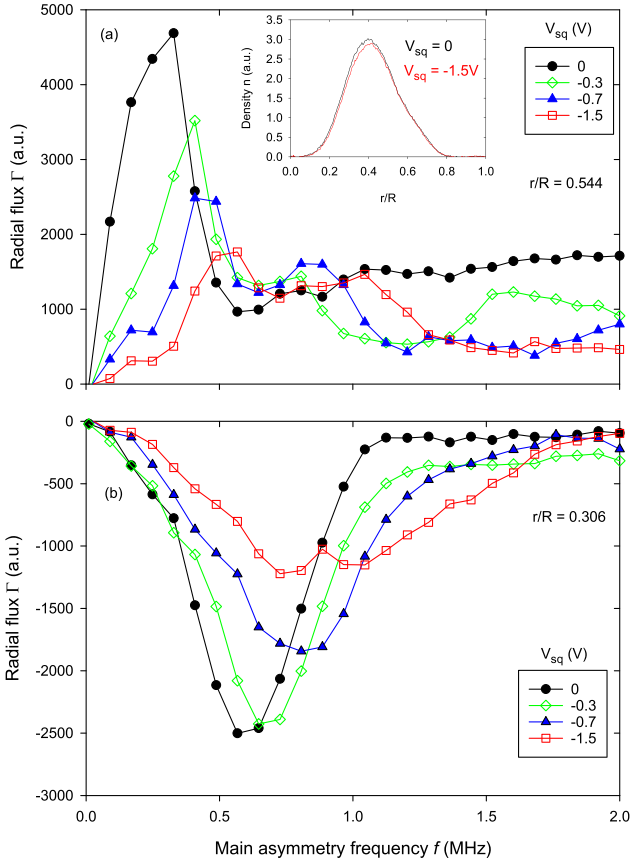


**FIG. 3.** Effect of a negative DC squeeze applied to the full ring S3 on the radial flux vs main asymmetry frequency curves for $\phi_{cw} = -60$ V. The legends show the value of the voltage applied to S3. (a) Results for the radius $r/R = 0.544$. The inset shows the electron density vs radius both with and without a squeeze applied (but without the main asymmetry), showing that this squeeze alone has little effect even at the largest squeeze magnitude. (b) Results for the radius $r/R = 0.306$. Approximate flux calibration for both curves and those following is 1000 a.u. $\approx 10^5$ cm$^{-2}$ s$^{-1}$.

## B. Asymmetric DC squeeze

We next present results where the squeeze voltage is applied asymmetrically to the two azimuthal halves of S3 (i.e., a positive DC voltage applied to the top half and a negative voltage to the bottom half). This choice is inspired by the "ruffled squeeze" used in the work of Kabantsev and co-workers,[12–14] although in their case the potential includes both symmetric and asymmetric contributions.

Typical data for this type of experiment are shown in Fig. 6. Here, we have chosen to show data at a larger radius (r/R = 0.820) and focused on lower asymmetry frequencies to show the appearance of a double peak in the flux vs frequency curves. The double peak structure has not been previously reported and is not understood but may be related to a similar behavior in our simulation work.[17] In any case, data taken at r/R = 0.544 show similar qualitative features but have a single peak. The lower radius data (r/R = 0.306) shown in Fig. 3(b) show little variation with squeeze voltage over this frequency range and are omitted from the plot.

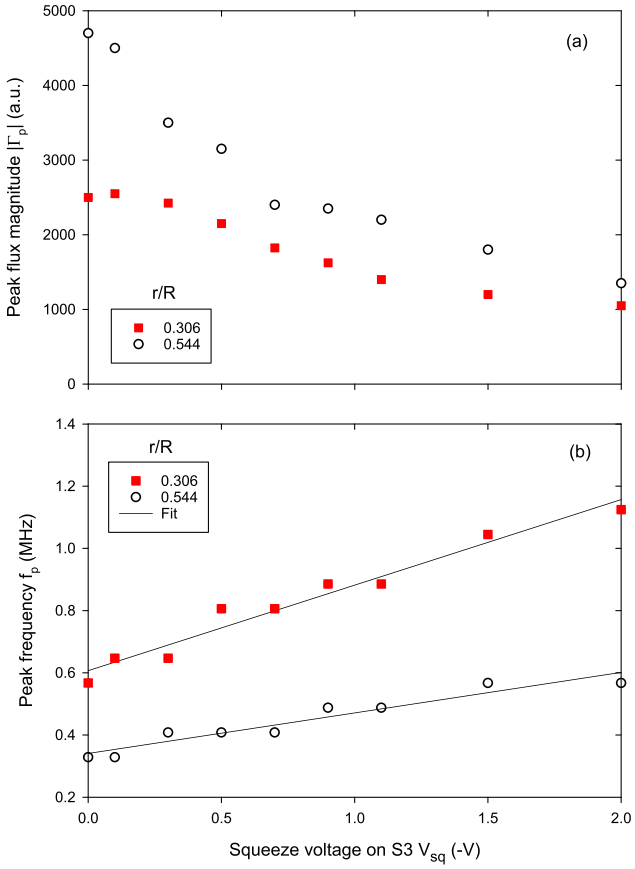


**FIG. 4.** Peak flux magnitude $|\Gamma_p|$ and peak frequency $f_p$ plotted vs the magnitude of the symmetric DC squeeze voltage $V_{sq}$ applied to S3 for the two chosen radii of Fig. 3: (a) peak flux magnitude $|\Gamma_p|$ and (b) peak frequency $f_p$.

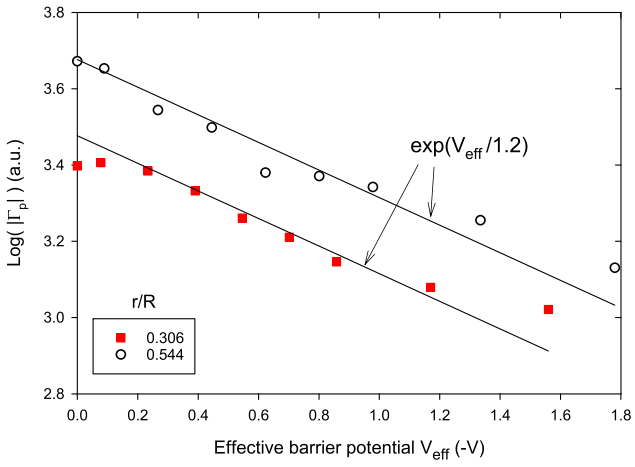


**FIG. 5.** The logarithm of $|\Gamma_p|$ vs the effective barrier potential $V_{eff}$. The solid lines show that the decrease in $|\Gamma_p|$ with $V_{eff}$ is given roughly by exp $(V_{eff}/1.2)$ for both radii.

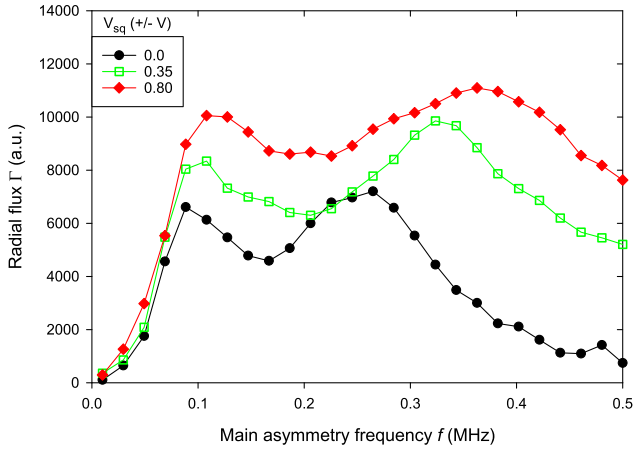


**FIG. 6.** Effect of an asymmetric DC squeeze applied to the two halves of ring S3 on the radial flux vs main asymmetry frequency curves for the radius $r/R = 0.820$. The legend shows the value of the voltage applied to S3.

Surprisingly, in this case, we find that the radial flux is *increased* with increasing magnitude of the squeeze voltage. This increase in the peak radial flux with squeeze magnitude is shown in Fig. 7(a) for both peaks. Again, we observe that the frequency $f_p$ of these peaks changes with squeeze voltage and this is shown in Fig. 7(b).

### C. Asymmetric AC squeeze

We have also explored the effect of applying the asymmetrical squeeze at various frequencies with the signal amplitude fixed at 0.1 V. This is shown in Fig. 8. For these cases, the peak flux is decreased by the application of the squeeze, although the amount of decrease depends on the squeeze frequency.

## IV. DISCUSSION

The results of Sec. III are offered primarily as an experimental contribution to the efforts to understand asymmetry-induced transport. While we are constrained by the lack of a detailed theory for our experiments, a number of comments on the results are in order. In the transport model we are considering, the transport is dominated by particles that are axially trapped in the main asymmetry potential. Transport occurs when these particles undergo collisions and become untrapped, now transiting the entire machine. The negative DC squeeze potential would prevent this from happening, so the decrease in radial flux seen in Figs. 3–5 makes qualitative sense. Because there is a separatrix between the trapped and passing particle distributions, however, a small change in the axial velocity is enough to move a particle from one population to the other. Since the asymmetry potential is of the order 0.2 V, we expect particles that have moved from trapped to transiting and back to have energies of that same order. The observed exponential scale of 1.2 V is, thus, larger than expected. If the reduction in $\Gamma_p$ with $V_{sq}$ is due to particles being excluded from trapped-to-untrapped transitions, then the particles involved must have a broader range of energies than our intuition suggests. We also note that the trapped particle model does not provide an obvious explanation for the shift in the peak frequency $f_p$ with squeeze voltage.

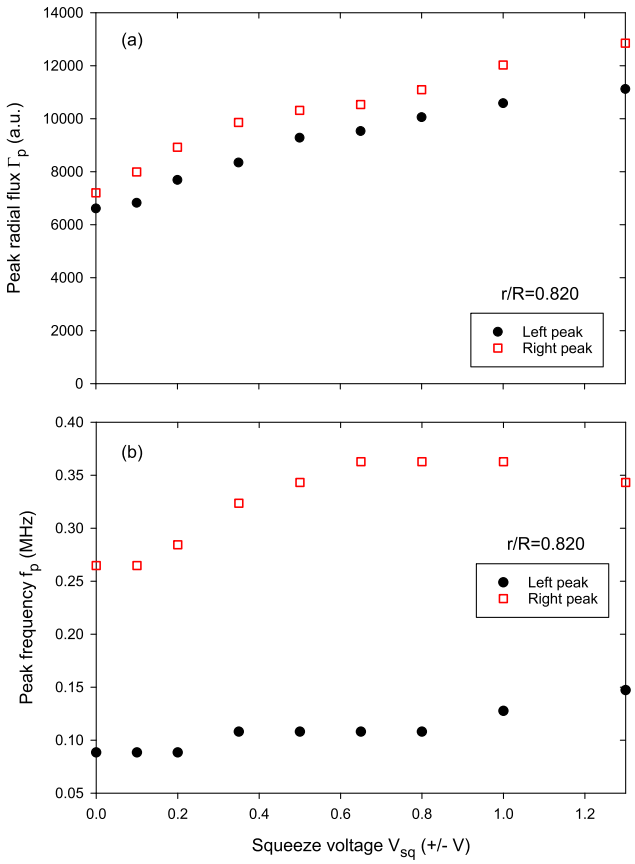


**FIG. 7.** Peak flux magnitude $|\Gamma_p|$ and peak frequency $f_p$ plotted vs the magnitude of the asymmetric DC squeeze voltage $V_{sq}$ applied to S3 for the radius $r/R = 0.820$ for the data of Fig. 6. The data for both peaks are plotted. (a) Peak flux magnitude $|\Gamma_p|$. (b) Peak frequency $f_p$.

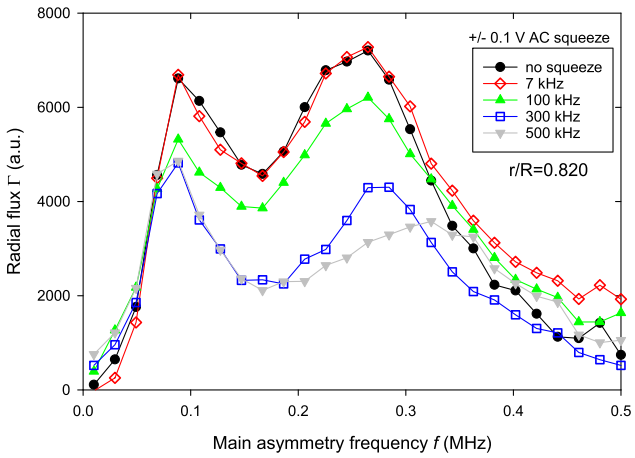


**FIG. 8.** Effect of an asymmetric AC squeeze applied to the two halves of ring S3 on the radial flux vs main asymmetry frequency curves for the radius $r/R = 0.820$. The legend shows the frequency of the voltage applied to S3.

An alternative interpretation of the symmetric DC squeeze data is that the primary effect of the squeeze is to gradually divide the experiment into two halves. It has long been known that shorter machines have less background transport,[20,21] presumably because the spectrum of background asymmetries is changed when the machine is made shorter.[22] Similarly, here, the spectrum and amplitude of our applied asymmetry [Eq. (1)] would be changed if the machine were halved, likely leading to reduced transport. Of course, the halving of the machine length in this experiment is done gradually as the squeeze voltage is made more negative so it is hard to quantify the effect.

Some support for this second interpretation is provided by the shifting of the peak frequency with squeeze voltage. In a previous paper[7] on the frequency dependence of the asymmetry-induced transport, it was noted that the peak frequencies increase with the axial mode number $k = n\pi/L$ of the asymmetry, where $L$ is the length of the plasma. Halving the plasma length would, thus, increase $k$, so the increase in the peak frequency observed here would be consistent with these previous results.

Turning now to the experiments with asymmetric squeezes (Secs. III B and III C), it is perhaps the most remarkable that in Fig. 6 the flux *increases* with the DC squeeze voltage, the opposite of the symmetric DC result. In similar experiments with a ruffled squeeze, Kabantsev and co-workers[12–14] have interpreted increases in transport as the result of induced chaotic particle orbits. It must be emphasized, however, that, for the asymmetric squeeze experiments, the squeeze is not just providing a barrier for axially transiting particles but also provides an applied asymmetry potential in addition to the main asymmetry provided by the other rings and specified by Eq. (1). It is not surprising, then, that altered transport might be observed, but the details of how the two asymmetries combine are unclear. Indeed, as Fig. 8 shows, the asymmetric AC squeezes *reduce* the transport.

Two additional experiments elucidate this complication. In Fig. 9, we show how the density profile is changed by the application of the asymmetric squeeze potential alone [i.e., without the main applied asymmetry producing Eq. (1)]. It is clear that, generally, the asymmetric squeeze alone does change the density profile more significantly than the symmetric squeeze alone (see the inset of Fig. 3) and that the profile changes depend on the frequency of the squeeze

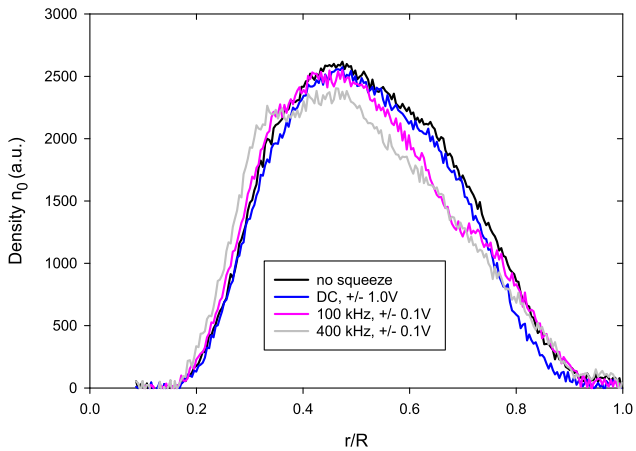


**FIG. 9.** Effect of the asymmetric squeeze alone on the electron density profile.

voltage. This is qualitatively consistent with our expectations for asymmetry-induced transport (see Fig. 2).

To address this, we have repeated the asymmetric squeeze experiments with the squeeze applied *before* the main asymmetry rather than simultaneously. The length of the squeeze is still 100 ms but is completed 1.3 ms before the main asymmetric potential is applied. The delay of 1.3 ms is short compared to the relaxation time of the density profile so changes produced by the squeeze will largely remain when the main asymmetry is applied but this squeeze cannot affect any trapped particle motion involved in the main asymmetry transport. As shown in Fig. 10, all types of squeeze now reduce the amount of transport produced by the main asymmetry. In particular, the increased flux previously observed for the asymmetric DC squeeze does not occur. Furthermore, we have compared the peak fluxes of the curves in Fig. 10 with the density gradient $-dn_0/dr$ at r/R = 0.820 obtained from density profiles of Fig. 9 and found a roughly linear relationship. Since we have previously noted[23] that the transport produced by our main asymmetry is largely diffusive (i.e., $\Gamma_p \propto dn_o/dr$), the following picture seems reasonable: The main effect of the asymmetric squeeze in these non-simultaneous experiments is to alter the density profile (and, thus, $dn_0/dr$), and the changes to the characteristic curves of the main asymmetry simply reflect this alteration. Further support for this interpretation comes from noting the magnitude of the squeeze voltage in Figs. 6–10. The asymmetric DC voltages required to produce an effect are much larger than the 0.1 V asymmetric AC voltage. Alternately, the 7 kHz case in Fig. 8 produces almost no change in the Γ vs $f$ curve. These observations are consistent with the general observation that there is little transport produced at low frequencies (see Fig. 2).

While illustrative, these non-simultaneous experiments do not allow us to resolve the relative roles of trapped particle dynamics and squeeze-induced profile modification in the simultaneous experiments of Secs. III B and III C. They do, however, support the idea that both effects must be included when interpreting such experiments. How to do this remains unclear at this time.

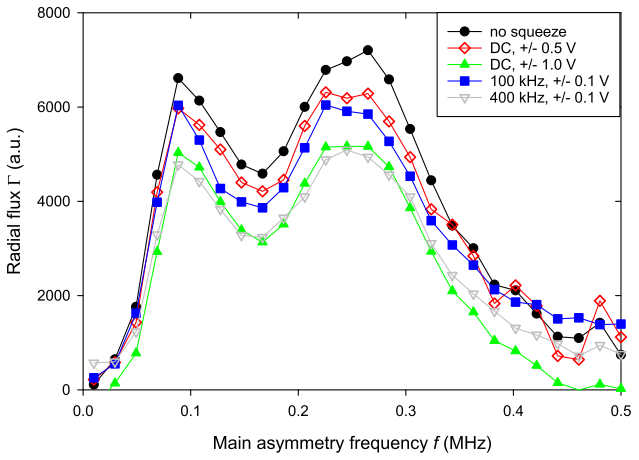


**FIG. 10.** Effect of various types of asymmetric squeeze applied to the two halves of ring S3 on the radial flux vs main asymmetry frequency curves for the radius $r/R = 0.820$ when the squeeze is applied before the asymmetry. The legend shows the types of squeeze applied to S3.

## V. CONCLUSIONS

The effect of various types of central barrier potentials on our characteristic flux vs frequency curves has been investigated. A negative symmetric DC squeeze applied to the entire central ring reduces the peak radial flux at both large and small radii by a factor $e^{(V_{eff}/1.2)}$ where $V_{eff}$ is the effective applied potential in volts. This squeeze also increases the frequency of this peak flux. The factor 1.2 is larger than expected from a trapped particle model and a qualitative alternative model is discussed. An asymmetric DC squeeze applied to the two azimuthal halves of the central electrode increases the peak radial flux as well as the peak frequency. An asymmetric AC squeeze applied to the two azimuthal halves of the central electrode decreases the peak radial flux. This holds true for all but the smallest AC frequencies. These asymmetric squeezes themselves produce radial transport. When the squeeze is applied before the main asymmetry, only reductions in the radial flux are observed. This suggests that, for the case of an asymmetric squeeze, density profile modification produced by the squeeze plays a role in the observed changes to our characteristic flux vs frequency curves. We have not yet found a way to distinguish between these effects and those caused by modification of axial particle motion.

## ACKNOWLEDGMENTS

This work was supported by the U.S. Department of Energy under Grant No. DE-FG02-06ER54882.

## AUTHOR DECLARATIONS

### Conflict of Interest

The authors have no conflicts to disclose.

### Author Contributions

**Dennis L. Eggleston:** Conceptualization (lead); Data curation (lead); Formal analysis (lead); Funding acquisition (lead); Investigation (lead); Methodology (lead); Project administration (lead); Resources (lead); Software (lead); Supervision (lead); Validation (lead); Visualization (lead); Writing – original draft (lead); Writing – review & editing (lead).

## DATA AVAILABILITY

The data that support the findings of this study are available from the author upon reasonable request.

## REFERENCES

[1]D. L. Eggleston, T. M. O'Neil, and J. H. Malmberg, Phys. Rev. Lett. **53**, 982 (1984).
[2]J. Notte and J. Fajans, Phys. Plasmas **1**, 1123 (1994).
[3]X.-P. Huang, F. Anderegg, E. M. Hollman, C. F. Driscoll, and T. M. O'Neil, Phys. Rev. Lett. **78**, 875 (1997).
[4]J. M. Kriesel and C. F. Driscoll, Phys. Rev. Lett. **85**, 2510 (2000).
[5]D. L. Eggleston and B. Carrillo, Phys. Plasmas **9**, 786 (2002).
[6]E. Gilson and J. Fajans, Phys. Rev. Lett. **90**, 015001 (2003).
[7]D. L. Eggleston and B. Carrillo, Phys. Plasmas **10**, 1308 (2003).
[8]J. R. Danielson and C. M. Surko, Phys. Rev. Lett. **94**, 035001 (2005).
[9]A. A. Kabantsev and C. F. Driscoll, Phys. Rev. Lett. **89**, 245001 (2002a).
[10]A. A. Kabantsev, J. H. Yu, R. B. Lynch, and C. F. Driscoll, Phys. Plasmas **10**, 1628 (2003).

[11]C. F. Driscoll, A. A. Kabantsev, T. J. Hilsabeck, and T. M. O'Neil, in *Non-Neutral Plasma Physics V*, edited by M. Schauer, T. Mitchell, and R. Nebel(American Institute of Physics, Melville, NY, 2003), p.3.
[12]A. A. Kabantsev, D. H. E. Dubin, C. F. Driscoll, and Yu. A. Tsidulko, Phys. Rev. Lett. **105**, 205001 (2010).
[13]D. H. Dubin, A. A. Kabantsev, and C. F. Driscoll, Phys. Plasmas **19**, 056102 (2012).
[14]C. F. Driscoll, A. A. Kabantsev, D. H. E. Dubin, and Yu. A. Tsidulko, in *Non-Neutral Plasma Physics VIII*, edited by X. Sarasola, L. Schweikhard, and T. S. Pedersen (American Institute of Physics, Melville, NY, 2013).
[15]D. L. Eggleston and T. M. O'Neil, Phys. Plasmas **6**, 2699 (1999).
[16]D. L. Eggleston, Phys. Plasmas **14**, 012302 (2007).
[17]D. L. Eggleston, Phys. Plasmas **19**, 042307 (2012).
[18]D. L. Eggleston, Phys. Plasmas **21**, 072318 (2014).
[19]D. L. Eggleston, K. J. McMurtry, A. A. Kabantsev, and C. F. Driscoll, Phys. Plasmas **13**, 032303 (2006).
[20]C. F. Driscoll, K. S. Fine, and J. H. Malmberg, Phys. Fluids **29**, 2015 (1986).
[21]D. L. Eggleston, Phys. Plasmas **4**, 1196 (1997).
[22]We note that, alternately, Ref. 11 claims the length effect itself is due to axial particle trapping.
[23]D. L. Eggleston, Phys. Plasmas **17**, 042304 (2010).